Modeling Multilayer Adsorption of Interacting Polyatomic Species on Heterogeneous Surfaces

F. O. Sánchez-Varretti [a,b], G. D. García [a,b], A. J. Ramirez-Pastor [a,1]

[a] *Dpto. de Física, Instituto de Física Aplicada, Universidad Nacional de San Luis - CONICET, Chacabuco 917, 5700 San Luis, Argentina.*

[b] *Universidad Tecnológica Nacional, Regional San Rafael, Gral. Urquiza 314, 5600, San Rafael, Mendoza, Argentina.*

Abstract

In the present work, a generalized lattice-gas model to study multilayer adsorption of interacting polyatomic species on heterogeneous surfaces is introduced. Using an approximation in the spirit of the well-known Brunauer–Emmet–Teller (BET) model, a new theoretical isotherm is obtained in one- and two-dimensional lattices and compared with Monte Carlo simulation. In addition, the BET approach is used to analyze these isotherms and to estimate the monolayer volume. In all cases, the application of the BET equation leads to an underestimate of the true monolayer capacity. However, significant compensation effects were observed for heterogeneous surfaces and attractive lateral interactions.

Key words: Equilibrium thermodynamics and statistical mechanics, Surface thermodynamics, Adsorption isotherms, Multilayer adsorption, Monte Carlo simulations

[1] Corresponding author. Fax +54-2652-430224, E-mail: antorami@unsl.edu.ar

1 Introduction

The theoretical description of adsorption is a long-standing complex problem in surface science that presently does not have a general solution [1–4].

In 1918 Langmuir derived an analytical expression for the monolayer adsorption isotherm corresponding to a non-interacting monoatomic gas on an homogeneous surface [5]. Later, some theories have been proposed to describe equilibrium adsorption in the multilayer regime [6–17]. Among them, the one of Brunauer-Emmett-Teller (BET) [6] and the one of Frenkel-Halsey-Hill [7–9] are the simplest which provide the basis to construct more elaborate approaches. Those more elaborate analytic approaches take into account lateral interactions between the admolecules, differences between the energy of the first and upper layers, surface energetic heterogeneity and so forth. These leading models have played an important role in the characterization of solid surfaces by means of gas adsorption.

A more accurate description of multilayer adsorption should account for the fact that, in practice, most adsorbates are polyatomic. Even the simplest nonspherical molecules such as N_2 and O_2 may adsorb on more than one site depending on the surface structure [17–23]. This effect, called multisite-occupancy adsorption, introduces a new complexity to the adsorption theory.

From a theoretical point of view, several attempts were done in the past in order to solve the problem of polyatomic species adsorbed on 2D substrates [24–33]. In general, these treatments are limited in their application because they are valid only for monolayer adsorption. There are few studies that take into account the effect of multisite occupancy in the multilayer regime [34–40]. Aranovich and Donohue [34,35] presented a multilayer adsorption isotherm that should be capable to include multisite occupancy. Later, a closed exact solution for the multilayer adsorption isotherm of dimers was reported [36,37].

There are another two important physical facts which have not been sufficiently studied: 1) the effect of lateral interactions between the ad-molecules and 2) the effect of surface heterogeneity in presence of multisite and multilayer adsorption. In the first case, a recent paper [38] extends the BET equation to include nearest-neighbor lateral interactions between the molecules adsorbed in the first layer. Following the configuration-counting procedure of the Bragg-Williams approach and the quasi-chemical approximation, Ref. [38] provides a simple statistical mechanical framework for studying multilayer adsorption of interacting polyatomics. In the second case, a recent job shows how the monolayer volume predicted by BET equation differs from its real value when considering both the adsorbate size and the surface topography [39].

On the other hand, combined effects coming from lateral interactions, multi-

site occupancy and surface heterogeneity have been analyzed in the interesting paper by Nikitas [40]. In Ref. [40], the author concluded that: (*i*) one can obtain an underestimation of the true monolayer capacity of the order of 25% when the adsorbate occupies more than one lattice site, (*ii*) this underestimation will become worse if the effect of the multisite occupancy is coupled with heterogeneity effects, and (*iii*) the attractive interactions in the gas adsorption lead always to a weak overestimation of the monolayer volume.

The previously discussed issues can be outlined in Fig. 1, where dimensions of complexity are sketched. In each axis, a particular characteristic of the adsorption process, that can (or cannot) be present in a particular model, is shown. Usually, the more features a model has, the more is its generality and more complex the process it describes. Fig. 1 shows models that include adsorption with lateral interactions, but they do not allow to multisite occupancy, or incorporate surface energetic heterogeneity, but they overlook lateral interactions in the adsorbed layer, etc. At present, some models venture in some of these dimensions of complexity but, the vast majority, lack the complete set of complexities. It is also clear that the farther away we are from the origin the more general (and usually the more complex) the model is. Even more, the upper plane (including multisite occupancy), is a set of models developed in the last decade that represents a leap forward in the lattice-gas theory.

In this work we will attempt to take one step further away from the origin, into a more general and encompassing scheme, presenting a model that considers the totality of these dimensions of complexity (multilayer adsorption, lateral interactions, multisite occupancy, energetic heterogeneity and surface topography). For this purpose, a theoretical formalism is presented based upon the analytical expression of the adsorption isotherm with lateral interaction weighted by the characteristic length of the surface heterogeneous. In addition, Monte Carlo (MC) simulations are performed in order to test the validity of the theoretical model. The new theoretical scheme allows us (1) to obtain an accurate approximation for multilayer adsorption on 2D substrates accounting multisite occupancy, lateral interactions, energetic heterogeneity and surface topography, and (2) to provide a simple model from which experiments may be reinterpreted.

2 Model and theory

In this section, we will present the model and make a revision of some existing theories describing the adsorption process in the framework of the lattice-gas approximation.

2.1 Model

The substrate is modeled by a regular lattice of M sites with periodic boundary conditions, where the adsorption energy of the first layer ε_i^f depends on each site i of the surface. The adsorbate is represented by k-mers (linear particles that have k identical units). A k-mer adsorbed occupies k sites of the lattice and can arrange in many configurations. This property is called multisite-occupancy adsorption.

On the other hand, for higher layers, the adsorption of a k-mer is exactly onto an already absorbed one, with an adsorption energy of $k\varepsilon$. Thus, the monolayer structure reproduces in the remaining layers. The mechanism used to describe the adsorption in the multilayer regime mimics the phenomenon called pseudomorphism. This phenomenon was observed, by using low-energy electron diffraction technique [41–43], in the case of adsorption of straight chain saturated hydrocarbon molecules on metallic surfaces.

Finally, and in order to obtain an approximation in the spirit of the BET model, attractive and repulsive lateral interactions are considered in the first layer and horizontal interactions are ignored in higher layers. As it is well-known [17,44], BET equations can be applied at coverage not greatly exceeding (statistically) monolayer coverage. In these conditions, the density of the molecules in the second and higher adlayers is expected to be much lower than that in the first adsorbed layer. Therefore, it seems to be satisfactorily enough to take into account only the interactions between the molecules adsorbed in the first layer. Under these considerations the Hamiltonian can be written as:

$$H = \sum_{i=1}^{M} \varepsilon_i^f \sigma_i + k\varepsilon(N - N_1) + w \sum_{\langle i,j \rangle} \sigma_i \sigma_j - wN_1(k-1), \tag{1}$$

where the first term of the right-hand side represents the adsorption energy of the N_1 k-mers adsorbed in the first layer (adjacent to the adsorbent) and the second term is the energy of the $(N - N_1)$ k-mers adsorbed on top of the first layer (second layer, third layer, and so on). The third and fourth terms correspond to the lateral interaction energy, where w is the interaction energy between two nearest-neighbor (NN) units belonging to different k-mers adsorbed in the first layer (we use $w > 0$ for repulsive and $w < 0$ for attractive interactions); σ_i is the occupation variable which can take the values 0 if the site i is empty or 1 if the site i is occupied and $\langle i, j \rangle$ represents pairs of NN sites. Since the summation in the third term overestimates the total energy by including $N_1(k-1)$ bonds belonging to the N_1 adsorbed k-mers, the fourth term subtracts this exceeding energy.

Our study will be restricted to the class of lattice-gas models in which the

substrate is a regular array of individual adsorption sites where molecules can be deposited (also in a discrete manner). In the following sections, some analytical deductions of those models will be reviewed. A more in depth treatment is carried out in the original publications.

2.2 Multilayer adsorption of non-interacting polyatomics on homogeneous surfaces

One way to begin our analysis is to review the behavior of a system of identical particles, which will be adsorbed on a regular lattice of M identical sites of adsorption [37]. The supposition is that, like in the BET model, adsorption is done on the surface of the solid or onto an already adsorbed particle. In this case, instead of adsorbing spherically symmetric ad-atoms, entities that occupy k consecutive lattice sites will be used.

Therefore, only two possible unit-adsorption processes can occur: (1) a k-mer occupies k consecutive empty surface sites; and (2) a k-mer adsorbs on top of an already adsorbed k-mer. This adsorptive process will form columns of k-mers on the solid. It must be noticed that a unit-adsorption where a k-mer adsorbs on top of two already adsorbed k-mers is prohibited.

In the case of the unit-desorption processes, only it will be able to desorb a k-mer that is on the top of one k-mers column or a k-mer that is adsorbed on the solid surface, but has no other k-mers adsorbed on top of it.

Under these conditions, the grand partition function of the system is:

$$\Xi = \sum_{n=0}^{n_{max}} \Omega_k(n, M)\xi^n, \tag{2}$$

where $n_{max}(= M/k)$ is the maximum number of columns that can be formed, $\Omega_k(n, M)$ is the total number of distinguishable configurations of n columns in M sites and ξ is the grand partition function of a unique column of k-mers that has at least one k-mer in the first layer.

On the other hand, the grand partition function of the monolayer (Ξ_1) is:

$$\Xi_1 = \sum_{n=0}^{n_{max}} \Omega_k(n, M)\lambda_1^n, \tag{3}$$

being n, in this case, the number of k-mers adsorbed on the surface of the solid (first layer), and λ_1 the fugacity of the monolayer. $\Omega_k(n, M)$ is still the

number of possible configurations with n k-mers in M sites. This quantity must be equal in Eqs. (2) and (3).

By comparing Eqs. (2) and (3) it is possible to observe that they have a similar form. This allows us to write:

$$\left(\frac{\partial \Xi}{\partial \xi}\right)_{M,T} = \left(\frac{\partial \Xi_1}{\partial \lambda_1}\right)_{M,T}. \tag{4}$$

Inspired by this similarity, the following ansatz can be proposed:

$$\lambda_1 = \xi. \tag{5}$$

Then

$$\lambda_1 = \xi = \frac{cp/p_0}{1 - p/p_0} \Rightarrow \frac{p}{p_0} = \frac{1}{1 + c/\lambda_1}, \tag{6}$$

where p/p_0 is the relative pressure [17,45] and $c = q_1/q = \exp[-\beta k(\varepsilon^f - \varepsilon)]$ is the ratio between the partition function of a particle in the first layer and a particle in any other layer [$\beta = (k_B T)^{-1}$, being k_B the Boltzmann constant]. And, then, the monolayer coverage can be written as:

$$\theta_1 = \frac{k\bar{n}}{M} = \frac{k}{M}\lambda_1 \left(\frac{\partial \ln \Xi_1}{\partial \lambda_1}\right)_{M,T} \tag{7}$$

$$= \frac{k}{M}\xi \left(\frac{\partial \ln \Xi}{\partial \xi}\right)_{M,T}, \tag{8}$$

where $\bar{n}$ is the mean number of k-mers adsorbed on the first layer.

Now, the total coverage (θ) can be written in terms of the coverage of the monolayer (θ_1):

$$\theta = \frac{\theta_1}{1 - p/p_0}. \tag{9}$$

The theoretical procedure in Eqs. (6)-(9) provides the isotherm in the multilayer regime from the isotherm in the monolayer regime. In fact:

(1) By using θ_1 as a parameter ($0 \leq \theta_1 \leq 1$), the relative pressure is obtained by using Eq. (6). This calculation requires the knowledge of an analytical expression for the monolayer adsorption isotherm.

(2) The values of θ_1 and p/p_0 are introduced in Eq. (9) and the total coverage is obtained. The items (1) and (2) are summarized in the following scheme:

$$\theta_1 + \lambda_1(\theta_1) + \text{Eq. (6)} \rightarrow p/p_0$$

$$\Rightarrow \theta_1 + p/p_0 + \text{Eq. (9)} \rightarrow \theta.$$

Following the previous scheme, it is possible to obtain the exact multilayer isotherm for k-mers in 1D homogeneous surfaces. In fact, in Ref. [37] the expression for the monolayer coverage is proved to be:

$$p/p_0 = \frac{\theta_1 \left[1 - \frac{(k-1)}{k}\theta_1\right]^{k-1}}{kc(1-\theta_1)^k + \left[1 - \frac{(k-1)}{k}\theta_1\right]^{k-1}}. \tag{10}$$

Equations (9) and (10) represent the exact solution of the 1D model and, as it is expected, retrieve the BET equation for the case $k = 1$.

Also, the previous scheme can be used to obtain an accurate approximation for multilayer adsorption on 2D substrates accounting for multisite occupancy. In this case, the semi-empirical monolayer adsorption isotherm [33,45] can be used

$$\frac{p}{p_0} = \frac{\theta_1 \left[1 - \frac{(k-1)}{k}\theta_1\right]^{(k-1)\theta_1} \left[1 - \frac{2(k-1)}{\zeta k}\theta_1\right]^{(k-1)(1-\theta_1)}}{mkc\,(1-\theta_1)^k + \theta_1 \left[1 - \frac{(k-1)}{k}\theta_1\right]^{(k-1)\theta_1} \left[1 - \frac{2(k-1)}{\zeta k}\theta_1\right]^{(k-1)(1-\theta_1)}}, \tag{11}$$

where ζ is the connectivity of the lattice and m represents the number of available configurations (per lattice site) for a linear k-mer at zero coverage. Thus, $m = 1$ for $k = 1$ and $m = \zeta/2$ for $k \geq 2$.

Note that, for $\zeta = 2$, Eq. (11) is identical to the Eq. (10). Therefore, Eqs. (9) and (11) represent the general solution of the problem of multilayer adsorption in homogeneous surfaces with multisite occupancy.

In the following section our aim will be to generalize this expression to include the lateral interactions following the methodology used in Ref. [38]. Clearly, the complexity of the isotherm is greatly increased, but the expression is still a manageable one and in the case of zero interactions the previous case is retrieved.

2.3 Multilayer adsorption of interacting polyatomics on homogeneous surfaces

Due to the complexity introduced in the analytical expressions because of the lateral interactions is that approximations are used to deal with this feature of the adsorption process. The most commonly used approximations are the mean-field approximation (MFA) [44,46] and the quasi-chemical approximation (QCA) [44,46]. The main assumption in MFA [QCA] is that sites [pairs of NN sites] are treated as if they were independent of each other [44].

As shown in previous work [46], the configuration-counting procedure of the QCA allows us to obtain an approximation that is significantly better than the MFA for polyatomics. Based on this finding, the rest of the discussion will be restricted to the estimates obtained under QCA.

In order to apply the theoretical scheme described in previous section, we start with the monolayer adsorption isotherm of interacting k-mers adsorbed on a lattice of connectivity ζ obtained from the formalism of QCA [46],

$$\lambda_1 = \left[\frac{\theta_1 \exp\left(\beta w z/2\right)}{k\ m\left(\frac{2}{\zeta}\right)^{2(k-1)}}\right] \times \left\{\frac{(1-\theta_1)^{k(\zeta-1)}\left[k-(k-1)\theta_1\right]^{k-1}\left[\frac{z\theta_1}{2k}-\alpha\right]^{z/2}}{\left[\frac{\zeta k}{2}-(k-1)\theta_1)\right]^{k-1}\left[\frac{\zeta}{2}(1-\theta_1)-\alpha\right]^{k\zeta/2}\left(\frac{z\theta_1}{\zeta k}\right)^{z}}\right\}, \tag{12}$$

where

$$z = \left[2(\zeta-1)+(k-2)(\zeta-2)\right], \tag{13}$$

$$\alpha = \frac{z\zeta}{2k}\frac{\theta_1(1-\theta_1)}{\left[\frac{\zeta}{2}-\left(\frac{k-1}{k}\right)\theta_1+b\right]}, \tag{14}$$

$$b = \left\{\left[\frac{\zeta}{2}-\left(\frac{k-1}{k}\right)\theta_1\right]^2-\frac{z\zeta}{k}A\theta_1(1-\theta_1)\right\}^{1/2}, \tag{15}$$

and

$$A = 1-\exp(-\beta w). \tag{16}$$

Replacing Eq. (12) into Eq. (6),

$$\left(\frac{p}{p_o}\right)^{-1} = 1 + \left\{\frac{ckm\left(\frac{2}{\zeta}\right)^{2(k-1)}\left[\frac{\zeta k}{2} - (k-1)\theta_1)\right]^{k-1}}{\theta_1 \exp\left(\beta w z/2\right)(1-\theta_1)^{k(\zeta-1)}}\right\} \times \left\{\frac{\left[\frac{\zeta}{2}(1-\theta_1) - \alpha\right]^{k\zeta/2}\left(\frac{z\theta_1}{\zeta k}\right)^{z}}{\left[k-(k-1)\theta_1\right]^{k-1}\left[\frac{z\theta_1}{2k} - \alpha\right]^{z/2}}\right\}. \quad (17)$$

Eqs. (9) and (17) represent the solution describing the multilayer adsorption of interacting k-mers on homogeneous surfaces in the framework of the QCA. This method is presented in more depth in [38].

In the next section, the role of surface heterogeneity and lateral interactions will be analyzed.

2.4 Multilayer adsorption of interacting polyatomics on heterogeneous surfaces

In the two previous sections, the multilayer isotherm was obtained from the monolayer isotherm. It is possible demonstrate that this formalism still holds for interacting k-mers and a given surface heterogeneity. However, this strategy leads to a complex solution that is not useful for practical purposes. To build a simpler function (easier to analyze), the multilayer heterogeneous isotherm will be approximated by a weighted sum of multilayer homogeneous isotherms.

The heterogeneous surface is modeled by two kinds of adsorption sites in the first layer (bivariate surface): strong sites with adsorption energy ε_1^f and weak sites with adsorption energy ε_2^f. As seen later, these sites can be spatially distributed in different ways (different topographies). Then, the total adsorption energy for an isolated k-mer on the first layer with k_1 monomers located over strong sites and k_2 monomers located over weak sites is

$$E_i = k_1\varepsilon_1^f + k_2\varepsilon_2^f. \quad (18)$$

Under these considerations, and using the formalism of the integral equation of the adsorption isotherm [17], the mean coverage θ can be written as

$$\theta = \sum_{E_i} f(E_i)\theta_{\text{loc}}(E_i), \quad (19)$$

where $f(E_i)$ is the fraction of k-uples of k_1 strong sites and k_2 weak sites ($k_1 + k_2 = k$) and $\theta_{\text{loc}}(E_i)$ represents the local multilayer adsorption isotherm corresponding to an adsorptive energy E_i. This local isotherm can be well

approximated by using the multilayer adsorption isotherm associated to an homogeneous surface characterized by an effective value of c given by

$$c_i = \exp\left[-\beta\left(E_i - k\varepsilon\right)\right]. \tag{20}$$

The value of c_i can also be expressed as function of c_1 and c_2, the values of c for homogeneous surfaces whose adsorption energies are ε_1^f and ε_2^f, respectively. Thus, if the i-th term in Eq. (19) corresponds to a k-mer with k_1 units located over strong sites and k_2 units located over weak sites, then

$$c_i = \left(c_1^{k_1} c_2^{k_2}\right)^{1/k}. \tag{21}$$

As an example, let us consider the multilayer adsorption of non-interacting dimers on a bivariate linear lattice, where strong and weak sites are spatially distributed in alternating homotattic patches of size l ($l = 1, 2, 3, \cdots$). In this case, Eq. (19) has three different terms, being each one of them a dimer isotherm with a particular value of c,

$$\begin{aligned}\theta = & \left(\frac{l-1}{2l}\right)\frac{1}{(1-p/p_0)}\left\{1-\left[\frac{1-p/p_0}{1+(4c_1-1)\,p/p_0}\right]^{1/2}\right\}+ \\ & +\left(\frac{1}{l}\right)\frac{1}{(1-p/p_0)}\left\{1-\left[\frac{1-p/p_0}{1+\left(4\sqrt{c_1c_2}-1\right)p/p_0}\right]^{1/2}\right\}+ \\ & +\left(\frac{l-1}{2l}\right)\frac{1}{(1-p/p_0)}\left\{1-\left[\frac{1-p/p_0}{1+(4c_2-1)\,p/p_0}\right]^{1/2}\right\}.\end{aligned} \tag{22}$$

The first [third] term in the RHS of Eq. (22) represents the adsorption within a strong [weak] patch, on a pair of sites $(\varepsilon_1^f, \varepsilon_1^f)$ $[(\varepsilon_2^f, \varepsilon_2^f)]$, with c_1 $[c_2]$. The fraction of $(\varepsilon_1^f, \varepsilon_1^f)$ $[(\varepsilon_2^f, \varepsilon_2^f)]$ pairs on the lattice is $(l-1)/2l$ [47]. The remaining term of Eq. (22) corresponds to a dimer isotherm on a $(\varepsilon_1^f, \varepsilon_2^f)$ [or $(\varepsilon_2^f, \varepsilon_1^f)$] pair ($c = \sqrt{c_1 c_2}$), being $1/l$ the fraction of this kind of pairs on the lattice. As it can be observed, Eq. (22) depends on l and the dimer isotherm *sees* the topography.

In general, the number of terms in Eq. (19) increases as the adsorbate size k is increased and this equation leads to a complex solution. This scheme can be notoriously simplified following the results in Ref. [39]. In this paper, the authors showed that:

- If $k \gg l$ (with $k > 1$), the multilayer adsorption isotherm can be represented by a single homogeneous isotherm

$$\theta = \theta_{\rm loc}\left(\sqrt{c_1 c_2}\right). \tag{23}$$

- For a topography where $k \ll l$, the isotherm is

$$\theta = \frac{1}{2}\theta_{\text{loc}}(c_1) + \frac{1}{2}\theta_{\text{loc}}(c_2). \tag{24}$$

- The details of the topography are relevant only when $k \sim l$. In this case, it is possible to consider a simpler expression of the multilayer isotherm given by

$$\theta = \left(\frac{l-1}{2l}\right)\theta_{\text{loc}}(c_1) + \left(\frac{1}{l}\right)\theta_{\text{loc}}(\sqrt{c_1 c_2}) + \left(\frac{l-1}{2l}\right)\theta_{\text{loc}}(c_2). \tag{25}$$

  Eq. (25) (i) captures the extreme behaviors Eqs. (23) and (24), and (ii) approximates very well the complete Eq. (19) in 1D and 2D. In the 2D case, the local isotherm in Eq. (25) is obtained from Eqs. (9) and (11), with $\zeta = 3$, 4 and 6 for honeycomb, square and triangular lattices, respectively.

Finally, in order to move toward a more general equation, we propose to extend Eq. (25) as to describe multilayer adsorption of interacting polyatomic molecules on heterogeneous surfaces. For this purpose, the local isotherms can be obtained from Eqs. (9) and (17). The advantages of using this simple description as a tool for interpreting multilayer adsorption data and characterization of the adsorption potential will be shown in Section 4 by analyzing simulation results.

3 Monte Carlo simulation

The adsorption process is simulated through a grand canonical ensemble MC method.

For a given value of the temperature T and chemical potential μ, an initial configuration with N k-mers adsorbed at random positions (on kN sites) is generated. Then, an adsorption-desorption process is started, where each elementary step is attempted with a probability given by the Metropolis [48] rule:

$$W = \min\{1, \exp[-\beta(\Delta H - \mu \Delta N)]\}. \tag{26}$$

ΔH and ΔN represent the difference between the Hamiltonians and the variation in the number of particles, respectively, when the system changes from an initial state to a final state. In the process there are four elementary ways to perform a change of the system state, namely, adsorbing one molecule onto the surface, desorbing one molecule from the surface, adsorbing one molecule in

the bulk liquid phase and desorbing one molecule from the bulk liquid phase. In all cases, $\Delta N = \pm 1$.

The algorithm to carry out one MC step (MCS), is the following :

1) Set the value of the chemical potential μ and the temperature T.
2) Set an initial state by adsorbing N molecules in the system. Each k-mer can adsorb in two different ways: i) on a linear array of (k) empty sites on the surface or ii) exactly onto an already adsorbed k-mer.
3) Introduce an array, denoted as Q, storing the coordinates of n_e entities, being n_e,

$$\begin{aligned} n_e = & \text{number of available adsorbed } k-\text{mers for desorption } (n_d) \\ & + \text{ number of available } k-\text{uples for adsorption } (n_a), \end{aligned} \tag{27}$$

where n_a is the sum of two terms: i) the number of k-uples of empty sites on the surface and ii) the number of columns of adsorbed k-mers (note that the top of each column is an available k-uple for the adsorption of one k-mer).
4) Choose randomly one of the n_e entities, and generate a random number $\chi \in [0, 1]$

4.1) if the selected entity is a k-uple of empty sites on the surface then adsorb a k-mer if $\chi \leq W_{ads}^{surf}$, being W_{ads}^{surf} the transition probability of adsorbing one molecule onto the surface.

4.2) if the selected entity is a k-uple of empty sites on the top of a column of height i, then adsorb a new k-mer in the $i+1$ layer if $\chi \leq W_{ads}^{bulk}$, being W_{ads}^{bulk} the transition probability of adsorbing one molecule in the bulk liquid phase.

4.3) if the selected entity is a k-mer on the surface then desorb the k-mer if $\chi \leq W_{des}^{surf}$, being W_{des}^{surf} the transition probability of desorbing one molecule from the surface.

4.4) if the selected entity is a k-mer on the top of a column then desorb the k-mer if $\chi \leq W_{des}^{bulk}$, being W_{des}^{bulk} the transition probability of desorbing one molecule from the bulk liquid phase.

5) If an adsorption (desorption) is accepted in 4), then, the array Q is updated.
6) Repeat from step 4) M times.

The first r MCS of each run were discarded to allow for equilibrium and the next r' MCS were used to compute averages. The total coverage was obtained as,

$$\theta = \frac{k \langle N \rangle}{M}, \tag{28}$$

where $\langle N \rangle$ is the mean number of adsorbed particles, and $\langle ... \rangle$ means the time average over the MC simulation runs.

4 Results and discussion

In the present section, the main characteristics of the multilayer adsorption isotherm given by Eq. (25) [with local isotherms obtained from Eqs. (9) and (17)] will be analyzed, in comparison with simulation results for a lattice-gas of interacting k-mers on heterogeneous one-dimensional and square lattices.

Heterogeneity is introduced by considering bivariate surfaces, i.e., surfaces composed by two kinds of sites in the first layer, strong and weak sites, with adsorptive energies ε_1^f and ε_2^f, respectively. Recent developments in the theory of adsorption on heterogeneous surfaces, like the supersite approach [49], and experimental advances in the tayloring of nanostructured adsorbates [50,51], encourage this kind of study. A special class of bivariate surfaces, with a chessboard structure, has been observed recently to occur in a natural system [52], although it was already intensively used in modeling adsorption and surface diffusion phenomena [47,53–55].

Bivariate surfaces may also mimic, to a rough approximation, more general heterogeneous adsorbates. Just to give a few examples, we may mention the surfaces with energetic topography arising from a continuous distribution of adsorptive energy with spatial correlations, like those described by the dual site-bond model [56], or that arising from a solid where a small amount of randomly distributed impurity (strongly adsorptive) atoms are added [57]. In both cases the energetic topography could be roughly represented by a random spatial distribution of irregular patches (with a characteristic size) of weak and strong sites.

In the particular case studied in this article, the surface is modeled in two different ways: (1) as a chain of alternating patches of size l (see Fig. 2a); and (2) as a collection of finite homotattic patches in a chessboard-like array, where each patch is assumed to be a domain of equal size, $l \times l$ sites (see Fig. 2b). In this model, the energy correlation length is simply given by the patch size.

The computational simulations have been developed for one-dimensional chains of 10^4 sites, and square $L \times L$ lattices with $L = 144$, and periodic boundary conditions (note that the linear dimension L has to be properly chosen in such a way that it is a multiple of l). In addition, the equilibrium state could be well reproduced after discarding the first $r \approx 10^6$ MCS. Then, averages were taken over $r' \approx 10^6$ MCS successive configurations. With these values of L, r and r', (1) finite-size effects are negligible and (2) statistical errors in Figs. 3-6 are smaller than the size of the symbols.

In the first place, the topography effects will be considered. Fig. 3 shows the behavior of the multilayer adsorption isotherms for $k = 2$, $\beta w = -1$

and different topographies in 1D as indicated. The energy difference between patches has been chosen to be high ($c_1 = 1000$ and $c_2 = 1$) in order to emphasize the effects of the surface heterogeneity. The different topographies have been identified as l_C for patches of size l, and *bp* for the case of a surface with two big patches ($l \to \infty$). Symbols represent simulation results and lines correspond to theoretical data [Eq. (25)]. It can be seen that all curves are contained between the two limit ones: the one corresponding to 1_C and the one corresponding to *bp*.

For $l = 1$, the adsorption energy of a dimer in the first layer is $\varepsilon_1^f + \varepsilon_2^f$ for all configuration. In this condition, the system corresponds to a 1D lattice-gas of interacting dimers on a homogeneous surface and, consequently, Eq. (25) is exact.

In general, for $l > 1$, Eq. (25) is approximate. For $l = 2$, the analytic isotherms agree very well with the simulation data. However, for p/p_0 ranging between 0 and 0.15, some differences between theoretical and numerical data are observed. This happens because Eq. (25) has been built assuming that the three different pairs of sites are filled simultaneously and independently. However, for $c_1 \gg c_2$, the real process occurs in 3 stages: (*i*) the pairs of sites $(\varepsilon_1^f, \varepsilon_1^f)$ are covered; (*ii*) the pairs $(\varepsilon_2^f, \varepsilon_2^f)$ begin to be filled and (*iii*) the multilayer is formed. Note that in the first stage all the pair of sites $(\varepsilon_1^f, \varepsilon_2^f)$ and $(\varepsilon_2^f, \varepsilon_1^f)$ are removed. For this regime, a better approximation can be obtained by a semisum of two isotherms with c_1 y c_2.

When $l = 3$, the agreement between the analytic isotherms and the simulation data is very good. In this case, the first stage does not eliminate all the pairs of sites $(\varepsilon_1^f, \varepsilon_2^f)$ and $(\varepsilon_2^f, \varepsilon_1^f)$, because each dimer occupies only two sites in the strong patches. For this reason, the range of validity of Eq. (25) is wider than in the previous case. Now, if $l = 4$ or $l = 5$, the behaviors are similar to those observed for $l = 2$ or $l = 3$, respectively. In general, for even l, the first stage eliminates almost completely the pairs of sites $(\varepsilon_1^f, \varepsilon_2^f)$ and $(\varepsilon_2^f, \varepsilon_1^f)$, while this does not happen for odd l. Finally, when $l \to \infty$, the fraction of pair $(\varepsilon_1^f, \varepsilon_2^f)$ and $(\varepsilon_2^f, \varepsilon_1^f)$ goes to zero and Eq. (25) is exact. This limit corresponds to the called large patches topography (*bp* surface in our model), where the surface is assumed to be a collection of homogeneous patches, large enough to neglect border effects between neighbor patches with different adsorption energies.

The effect of the lateral interactions on the behavior of the system will now be analyzed. For this purpose, Fig. 4 shows the adsorption isotherms for $k = 2$, $c_1 = 1000$, $c_2 = 1$ and two different values of the lateral interactions $\beta w = -1$ (attractive case) and $\beta w = 1$ (repulsive case). In addition, for each value of βw, the limit topographies (1_C and *bp*) have been considered (as seen in Fig. 3, all curves corresponding to all topographies are contained between them).

For repulsive couplings, the interactions do not favor the adsorption on the first layer and the isotherms shift to higher values of pressure. On the other hand, attractive lateral interactions facilitate the formation of the monolayer. Consequently, the isotherms shift to lower values of p/p_o and their slope increases as the ratio $|\beta w|$ increases. In both cases ($\beta w = -1$ and $\beta w = 1$), the agreement between theoretical and simulation data is excellent.

From the curves in Fig. 4 (and from data not shown here for the sake of clarity) it is observed that: there exists a wide range of βw's ($-2 \leq \beta w \leq 2$), where the theory provides an excellent fitting of the simulation data. In addition, most of the experiments in surface science are carried out in this range of interaction energy. Then, the present theory not only represents a qualitative advance in the description of the multilayer adsorption of interacting k-mers on heterogeneous surfaces, but also gives a framework and compact equations to consistently interpret thermodynamic multilayer adsorption experiments of polyatomics species such as alkanes, alkenes, and other hydrocarbons on regular surfaces.

The effect of energetic heterogeneity (ratio between c_1 and c_2) is analyzed in Fig. 5, where the degree of heterogeneity is varied by changing the value of c_2 between 1 and 100 with c_1 fixed ($c_1 = 1000$). As in Fig. 4, $k = 2$ and $\beta w = -1$. Lines represent theoretical results and symbols correspond to simulation data ($c_2 = 1$: circles; $c_2 = 10$: triangles; and $c_2 = 100$: squares). For each set of values of the parameters, the limit cases corresponding to 1_C (open symbols) and *bp* (solid symbols) topographies are studied. As it can be observed from the simple inspection of the figure, the effect of topography is important in a range of c_2/c_1 between 10^{-3} and 10^{-2} and is practically negligible for $10^{-1} < c_2/c_1 < 1$.

To complete the discussion started in Fig. 3, the effect of the k-mer size on the adsorption isotherms was evaluated. This study is shown in Fig. 6, where the 1_C and *bp* multilayer adsorption isotherms are plotted for $\beta w = -1$, $c_1 = 1000$, $c_2 = 1$ and two different values of k ($k = 2$ and $k = 10$). One important conclusion can be drawn from the figure. Namely, the effects of topography and energetic heterogeneity tend to disappear as the size k is increased.

The study in Figs. 3-6 was repeated for surfaces in 2D. The behavior of the curves (not shown here for brevity) is very similar to the one observed in 1D.

Summarizing, it has been shown that just by using an expression of three terms, Eq. (25), the multilayer adsorption of interacting polyatomics on 1D and 2D heterogeneous surfaces can be well approximated. In the next, this approximation and Monte Carlo simulations will be used to study how lateral interactions, multisite occupancy and surface heterogeneity affect the determination of monolayer volume predicted by the BET equation.

In a typical experiment of adsorption, the adsorbed volume of the gas, v, is measured at different pressures and at a given fixed temperature, the total coverage is $\theta = v/v_{\mathrm{m}}$. Analyzing an isotherm with the BET equation

$$\theta = \left(\frac{1}{1-p/p_0}\right)\left(\frac{cp/p_0}{1-p/p_o+cp/p_0}\right), \tag{29}$$

it is possible to estimate the monolayer volume if we rewrite the previous equation as:

$$\frac{p/p_0}{v\,(1-p/p_0)} = \frac{1}{cv_{\mathrm{m}}} + \frac{(c-1)}{cv_{\mathrm{m}}}p/p_0. \tag{30}$$

This equation is a linear function of p/p_0. If we denote with i and s, the y-intercept and the slope of this straight line, respectively, we obtain

$$v_{\mathrm{m}}^{*} = \frac{1}{i+s} \tag{31}$$

and

$$c^{*} = \frac{s}{i} + 1. \tag{32}$$

The asterisk has been added in order to indicate that the quantities given by Eqs. (31) and (32) correspond to the prediction of the BET theory. Then, by means of a plot (the so-called BET plot) of the experimental data of $\frac{p/p_0}{v(1-p/p_0)}$ vs p/p_0, an estimate of the monolayer volume and the parameter c can be obtained. Nevertheless, in the experiments it is commonly found that there are deviations from linearity in the BET plot.

Following the scheme described in previous paragraphs, numerical experiments were carried out to determine, in different adsorption situations, how much the value of the monolayer volume predicted by the BET equation differs from its real value, v_{m}. With this purpose, analytic and simulation isotherms were analyzed as experimental data. In addition, according to the recommendation of the Commission on Colloid and Surface Chemistry of the International Union of Pure and Applied Chemistry (IUPAC), the range chosen for the linear fit of Eq. (30) was $0.05 < p/p_0 < 0.30$ [58]. Under these conditions, the values obtained for the linear correlation coefficient were of the order of 0.99 and the standard errors in the intercept and slope allowed us to estimate the monolayer volume with an error less than 3 %. In this way, it has been determined how adsorbate size, surface heterogeneity and lateral interactions, affect the standard determination of the monolayer volume.

In Fig. 7, the calculated value of $v_{\mathrm{m}}^{*}/v_{\mathrm{m}}$ is plotted as a function of k for fixed values of c_1 and c_2 (namely $c_1 = 1000$ and $c_2 = 1$) and different values of the attractive lateral interaction. The repulsive interactions, not shown in the figure, show a marked deviation from the predicted BET equation, therefore wiping out compensation effects due to the surface heterogeneity.

Three sets of plots can be distinguished in Fig. 7. Each set (1) is the result of the effect of different lateral interactions strengths: $\beta w = 0$, circles; $\beta w = -0.5$, squares and $\beta w = -1.0$, triangles; and (2) depicts the limiting cases for the surface topography: open and solid symbols correspond to 1_C and *bp* surfaces, respectively. All other topographies must lay in between those two plots.

The behavior of the open symbols corresponds, essentially, to the behavior of the homogenous case [39], where an already known feature can be distinguished: the compensation effect of k is lower as k increases, as [37] stated for the non-interacting case. On the other hand, for *bp* surfaces, the compensation effect increases with k as seen in [39]. In all cases, for stronger (attractive) interaction strength the plots move upwards showing greater compensation effects.

As shown in previous work [36,37] for non-interacting k-mers on homogeneous surfaces, the monolayer volume from the BET model diminishes with increasing values of the k-mer size. The data presented in Fig. 7 demonstrate that attractive lateral interactions and surface heterogeneity play a key role in the compensation of k-mer size effects. This finding is very important because most of the experiments in surface science are carried out in these conditions.

Finally, the study in Fig. 7 was repeated for 2D surfaces (see Fig. 8). In this case, both the compensation effect for attractive interactions and the underestimation of the monolayer volume for repulsive interactions (not shown here) are more important than in the 1D case. The explanation is simple: in 1D systems, particles will interact only at their ends, regardless of k; on the other hand, in 2D systems, each particle interacts at their ends, but also interacts along its k monomers. This makes the interaction energy grow linearly with k (if all first neighbors are occupied), and indicates that lateral interactions play a more important role in two-dimensional adsorption systems than in one-dimensional ones.

5 Conclusions

In this work, the multilayer adsorption of interacting polyatomic molecules onto heterogeneous surfaces has been studied. The polyatomic character of

the adsorbate was modeled by a lattice gas of k-mers. With respect to the lateral interactions, the adsorbate-adsorbate couplings in the monolayer were explicitly considered in the theory. The range of validity of the analytical isotherms was analyzed by comparing theoretical and MC simulation results.

The 1D and 2D BET plots, obtained from theoretical and simulation isotherms, were also analyzed. For non-interacting k-mers, it was found that the use of BET equation leads to an underestimate of the true monolayer volume: this volume diminishes as k is increased. The situation is different for the case of interacting molecules over heterogeneous surface. Thus, attractive lateral interactions favor the formation of the monolayer and, consequently, compensate the effect of the multisite occupancy. In this case, the monolayer volume predicted by BET equation agrees very well with the corresponding true value. In the case of repulsive couplings, the lateral interactions impede the formation of the monolayer and the BET predictions are bad (even worse than those obtained in the non-interacting case). Both the compensation effect for attractive interactions and the underestimation of the monolayer volume for repulsive interactions are more important for 2D systems.

ACKNOWLEDGMENTS

This work was supported in part by CONICET (Argentina) under project number PIP 112-200801-01332; Universidad Nacional de San Luis (Argentina) under project 322000; Universidad Tecnológica Nacional, Facultad Regional San Rafael (Argentina) under projects PQPRSR 858 and PQCOSR 526 and the National Agency of Scientific and Technological Promotion (Argentina) under project 33328 PICT 2005.

Nomenclature

k	Adsorbate size
L	Lattice side
M	Total number of lattice sites
w	Interaction energy between two NN units belonging to different k-mers adsorbed in the first layer
$\langle i, j \rangle$	Pair of NN sites i, j
N	Total number of adsorbed k-mers
N_1	Number of k-mers adsorbed in the first layer
H	Hamiltonian of the system
n	Total number of k-mers columns on the lattice
$\bar{n}$	Mean number of k-mers columns on the lattice
n_{max}	Maximum number of columns that can be formed in M sites
T	Temperature
q_1	Partition function of a particle in the first layer
q	Partition function of a particle in the second and higher layers
c	Ratio between q_1 and q
p	Equilibrium gas pressure
p_0	Saturation vapor pressure of the gas
k_B	Boltzmann constant
m	Number of available configurations (per lattice site) for a linear k-mer at zero coverage
z	Parameter introduced in Eq. (13)
b	Parameter introduced in Eq. (15)
A	Parameter introduced in Eq. (16)
k_1	Number of units located over strong sites belonging to a k-mer adsorbed on the first layer of a bivariate surface
k_2	Number of units located over weak sites belonging to a k-mer adsorbed on the first layer of a bivariate surface

E_i	Adsorption energy corresponding to a k-mer adsorbed on the first layer of a bivariate surface with k_1 units located over strong sites and k_2 units located over weak sites, Eq. (18)
$f(E_i)$	Fraction of k-uples of k_1 strong sites and k_2 weak sites
c_1	Value of c for a homogeneous surface whose adsorption energy in the first layer is ε_1^f
c_2	Value of c for a homogeneous surface whose adsorption energy in the first layer is ε_2^f
c_i	Parameter introduced in Eqs. (20) and (21)
l	Patch size of the bivariate surface
n_d	Number of available adsorbed k-mers for desorption
n_a	Number of available k-uples for adsorption
n_e	Sum of n_d and n_a
Q	Array storing the coordinates of the n_e entities
W_{ads}^{surf}	Metropolis transition probability of adsorbing one molecule onto the surface
W_{ads}^{bulk}	Metropolis transition probability of adsorbing one molecule in the bulk liquid phase
W_{des}^{surf}	Metropolis transition probability of desorbing one molecule from the surface
W_{des}^{bulk}	Metropolis transition probability of desorbing one molecule from the bulk liquid phase
MCS	Monte Carlo step
r	Number of MCS to reach the equilibrium state
r'	Number of MCS to calculate the temporal average of the surface coverage
l_C	Symbol identifying a bivariate surface characterized by alternating patches of size l
bp	Symbol identifying a bivariate surface characterized by two big patches ($l \to \infty$)

v Adsorbed volume of gas

v_{m} Volume of gas required to form a monolayer

i y-intercept of the linearized form of the BET adsorption isotherm equation

s Slope of the linearized form of the BET adsorption isotherm equation

v_{m}^{*} Parameter introduced in Eq. (31)

c^{*} Parameter introduced in Eq. (32)

Greek symbols

ζ	Lattice connectivity
ε_i^f	Adsorption energy of the i-th site in the first layer
ε	Adsorption energy of a site in the second and higher adlayers
σ_i	Occupation variable of the site i
Ξ	Grand partition function of the system
$\Omega_k(n, M)$	Total number of distinguishable configurations of n columns in M sites
ξ	Grand partition function of a unique column of k-mers that has at least one k-mer in the first layer
Ξ_1	Grand partition function of the monolayer
λ_1	Fugacity of the monolayer
μ	Chemical potential
β	Inverse of the temperature in k_B units $[\beta = (k_B T)^{-1}]$
θ	Total surface coverage
θ_1	Surface coverage of the monolayer
α	Parameter introduced in Eq. (14)
ε_1^f	Adsorption energy of the strong sites in the first layer of a bivariate surface
ε_2^f	Adsorption energy of the weak sites in the first layer of a bivariate surface
$\theta_{\mathrm{loc}}(E_i)$	Local multilayer adsorption isotherm corresponding to an adsorptive energy E_i
χ	Random number between 0 and 1

Figure Captions

Fig. 1: Schematic representation of the evolution of complexity in the theoretical adsorption models.

Fig. 2: Schematic representation of heterogeneous bivariate square surfaces with chessboard topography. The black (white) symbols correspond to strong (weak) adsorption sites. (a) One-dimensional lattice and (b) square lattice. The patch size in this figure is $l = 2$.

Fig. 3: Adsorption isotherms for dimers on 1D lattices with $\beta w = -1$ and different topographies 1D as indicated. The energy difference between different patches has been chosen to be high ($c_1 = 1000$ and $c_2 = 1$) in order to emphasize the effects of the surface heterogeneity. Solid lines and symbols represent theoretical and simulation results, respectively. For each set of values of the parameters, the limit cases corresponding to 1_C (open symbols) and *bp* (solid symbols) topographies are shown.

Fig. 4: Adsorption isotherms for dimers on 1D lattices with $c_1 = 1000$, $c_2 = 1$ and two different values of the lateral interactions $\beta w = -1$ (attractive case) and $\beta w = 1$ (repulsive case). Solid lines and symbols represent theoretical and simulation results, respectively. For each set of values of the parameters, the limit cases corresponding to 1_C (open symbols) and *bp* (solid symbols) topographies are shown.

Fig. 5: Adsorption isotherms for dimers on 1D lattices with $\beta w = -1$. The degree of the surface heterogeneity is varied by changing the value of c_2 between 1 and 100 with c_1 fixed ($c_1 = 1000$). Lines represent theoretical results and symbols correspond to simulation data ($c_2 = 1$: circles; $c_2 = 10$: triangles; and $c_2 = 100$: squares). For each set of values of the parameters, the limit cases corresponding to 1_C (open symbols) and *bp* (solid symbols) topographies are shown.

Fig. 6: Adsorption isotherms for dimers on 1D lattices with $\beta w = -1$, $c_1 = 1000$, $c_2 = 1$ and two different values of k ($k = 2$ and $k = 10$). Solid lines and symbols represent theoretical and simulation results, respectively. For each set of values of the parameters, the limit cases corresponding to 1_C (open symbols) and *bp* (solid symbols) topographies are shown.

Fig. 7: Results of the BET plots for the adsorption in 1D heterogeneous surfaces with $c_1 = 1000$, $c_2 = 1$. Dependence on k of the fraction $v_{\mathrm{m}}^*/v_{\mathrm{m}}$ for three different values of βw: $\beta w = 0$, circles; $\beta w = -0.5$, squares and $\beta w = -1.0$, triangles. For each set of values of the parameters, the limit cases corresponding to 1_C (open symbols) and *bp* (solid symbols) topographies are shown.

Fig. 8: As Fig. 7 for 2D surfaces: $\beta w = 0$, circles; $\beta w = -0.1$, squares and $\beta w = -0.5$, triangles. Symbols connected by (solid) dotted lines correspond to results obtained from (theoretical) MC simulation isotherms.

References

[1] A. Clark, The Theory of Adsorption and Catalysis, Academic Press, New York and London, 1970.

[2] W.A. Steele, The interaction of gases with solid surfaces, Pergamon Press, New York, 1974.

[3] S.J. Gregg, K.S.W. Sing, Adsorption, Surface Area, and Porosity, Academic Press, New York, 1991.

[4] A.W. Adamson, Physical Chemistry of Surfaces, John Wiley and Sons, New York, 1990.

[5] I. Langmuir, J. Am. Chem. Soc. 40 (1918) 1361.

[6] S. Brunauer, P.H. Emmet, E. Teller, J. Am. Chem. Soc. 60 (1938) 309.

[7] J. Frenkel, Kinetic Theory of Liquids, Clarendon Press, Oxford, 1946; Dover reprint, New York, 1955.

[8] G.D.J. Halsey, Chem. Phys. 16 (1948) 931.

[9] T.L. Hill, Adv. Catal. 4 (1952) 211.

[10] W.G. McMillan, E. Teller, J. Chem. Phys. 19 (1951) 25.

[11] W.G. McMillan, E. Teller, J. Phys. Colloid Chem. 55 (1951) 17.

[12] B. Dreyfus, D. Deloche, M. Laloë, Phys. Rev. B 9 (1974) 1268.

[13] J. Cortés, P. Araya, J. Coll. Interface Sci. 115 (1987) 271.

[14] S.H. Payne, H.A. McKay, H.J. Kreuzer, M. Gierer, H. Bludau, H. Over, G. Ertl, Phys. Rev. B 54 (1996) 5073.

[15] S. B. Casal, H. S. Wio, S. Mangioni, Physica A 311 (2002) 443.

[16] K. Grabowski, A. Patrykiejew, S. Sokolowski, Surf. Sci. 506 (2002) 47.

[17] W. Rudziński and D. Everett, Adsorption of Gases on Heterogeneous Surfaces, Academic Press, New York, 1992.

[18] P. Zeppenfeld, J. George, V. Diercks, R. Halmer, R. David, G. Cosma, A. Marmier, C. Ramseyer, C. Girardet, Phys. Rev. Lett. 78 (1997) 1504.

[19] O.G. Mouritsen, A.J. Berlinsky, Phys. Rev. Lett. 48 (1982) 181.

[20] D. Ferry, J. Suzanne, Surf. Sci. 345 (1996) L19.

[21] J.W. He, C.A. Estrada, J.S. Corneille, M.C. Wu, D.W. Goodman, Surf. Sci. 261 (1992) 164.

[22] V. Panella, J. Suzanne, P.N.M. Hoang, C. Girardet, J. Phys. I 4 (1994) 905.

[23] D.L. Meixner, D.A. Arthur, S.M. George, Surf. Sci. 261 (1992) 141.

[24] L. Onsager, Ann. N. Y. Acad. Sci. 51 (1949) 627.

[25] B.H. Zimm, J. Chem. Phys. 14 (1946) 164.

[26] A. Isihara, J. Chem. Phys. 18 (1950) 1446; J. Chem. Phys. 19 (1951) 1142.

[27] P.J. Flory, J. Chem. Phys. 10 (1942) 51. P.J. Flory, Principles of Polymers Chemistry, Cornell University Press, Ithaca, NY, 1953.

[28] M.L. Huggins, J. Phys. Chem. 46 (1942) 151. M.L. Huggins, Ann. N.Y. Acad. Sci. 41 (1942) 1. M.L. Huggins, J. Am. Chem. Soc. 64 (1942) 1712.

[29] A.J. Ramirez-Pastor, T.P. Eggarter, V.D. Pereyra, J.L. Riccardo, Phys. Rev. B 59 (1999) 11027.

[30] A.J. Ramirez-Pastor, J.L. Riccardo, V. Pereyra, Langmuir 16 (2000) 10167.

[31] F. Romá, A.J. Ramirez-Pastor, J.L. Riccardo, Langmuir 19 (2003) 6770.

[32] J.L. Riccardo, F. Romá, A.J. Ramirez-Pastor, Phys. Rev. Lett. 93 (2004) 186101.

[33] J.L. Riccardo, F. Romá, A.J. Ramirez-Pastor, Int. J. Mod. Phys. B 20 (2006) 4709.

[34] G.L. Aranovich, M.D. Donohue, J. Colloid Interface Sci. 175 (1995) 492.

[35] G.L. Aranovich, M.D. Donohue, J. Colloid Interface Sci. 189 (1997) 101.

[36] J.L. Riccardo, A.J. Ramirez-Pastor, F. Romá, Langmuir 18 (2002) 2130.

[37] F. Romá, A.J. Ramirez-Pastor, J.L. Riccardo, Surf. Sci. 583 (2005) 213.

[38] G.D. García, F.O. Sánchez-Varretti, F. Romá, A.J. Ramirez-Pastor, Surf. Sci. 603 (2009) 980.

[39] F.O. Sánchez-Varretti, G.D. García, A.J. Ramirez-Pastor, F. Romá, J. Chem. Phys. 130 (2009) 194711.

[40] P. Nikitas, J. Phys. Chem. 100 (1996) 15247.

[41] L.E. Firment, G.A. Somorjai, J. Chem. Phys. 66 (1976) 2901.

[42] L.E. Firment, G.A. Somorjai, J. Chem. Phys. 69 (1978) 3940.

[43] G.A. Somorjai, M.A. Van Hove, Adsorbed Monolayers on Solid Surfaces, Springer-Verlag, Berlin, 1979.

[44] T. L. Hill, Statistical Mechanics, McGraw-Hill, New York, 1965; An Introduction to Statistical Thermodynamics, Addison Wesley Publishing Company, Reading, MA, 1960.

[45] F. Romá, J.L. Riccardo, A.J. Ramirez-Pastor, Langmuir 22 (2006) 3192.

[46] M. Dávila, F. Romá, J. L. Riccardo, A. J. Ramirez-Pastor, Surf. Sci. 600 (2006) 2011.

[47] F. Bulnes, A.J. Ramirez-Pastor, G. Zgrablich, Phys. Rev. E 65 (2002) 031603.

[48] N. Metropolis, A.W. Rosenbluth, M.N. Rosenbluth, A.H. Teller, E. Teller, J. Chem. Phys. 21 (1953) 1087.

[49] W.A. Steele, Langmuir 15 (1999) 6083.

[50] M.X. Yang, D.H. Gracias, P.W. Jacobs, G. Somorjai, Langmuir 14 (1998) 1458.

[51] G.P. Lopinski, D.D.M. Wayner, R.A. Wolkow, Nature (London) 406 (2000) 48.

[52] T.W. Fishlock, J.B. Pethica, R.G. Eydell, Surf. Sci. 445 (2000) L47.

[53] A.J. Ramirez-Pastor, F. Bulnes, G. Zgrablich, Surf. Sci. 536 (2003) 97.

[54] F. Romá, F. Bulnes, A.J. Ramirez-Pastor, G. Zgrablich, Phys. Chem. Chem. Phys. 5 (2003) 3694.

[55] F. Bulnes, A.J. Ramirez-Pastor, J.L. Riccardo, G. Zgrablich, Surf. Sci. 600 (2006) 1917.

[56] G. Zgrablich, C. Zuppa, M. Ciacera, J.L. Riccardo, W.A. Steele, Surf. Sci. 356 (1996) 257.

[57] F. Bulnes, F. Nieto, V. Pereyra, G. Zgrablich, C. Uebing, Langmuir 15 (1999) 5990.

[58] IUPAC, Commission on Colloid and Surface Chemistry of the International Union of Pure and Applied Chemistry, Pure Appl. Chem. 57 (1985) 603.

Figure 1

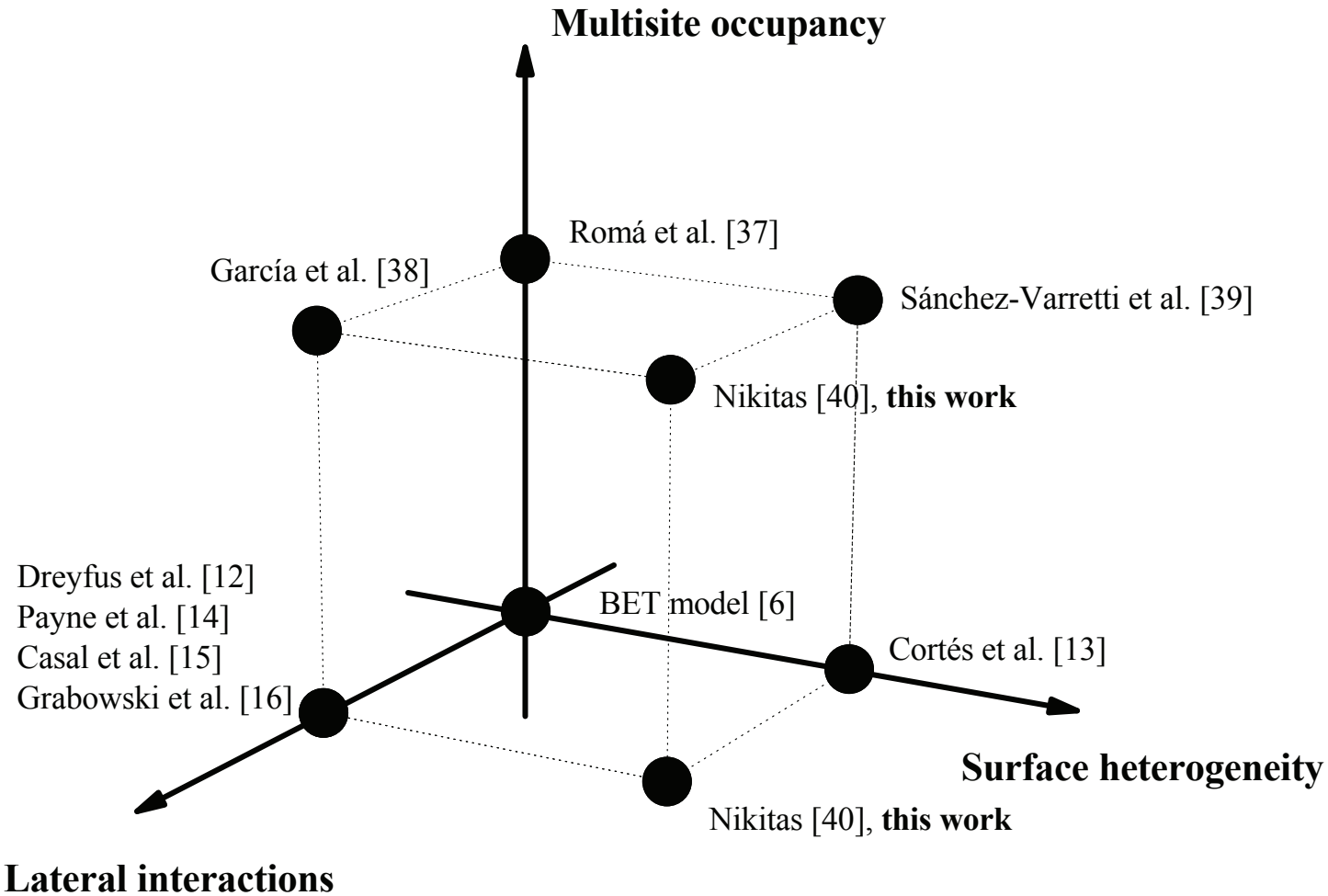

Fig. 1: Sánchez-Varretti et al.

Figure 2

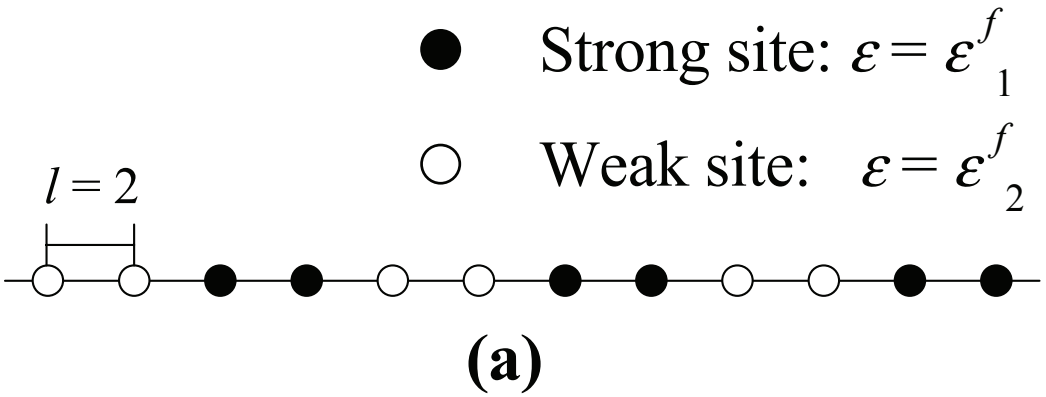

(a)

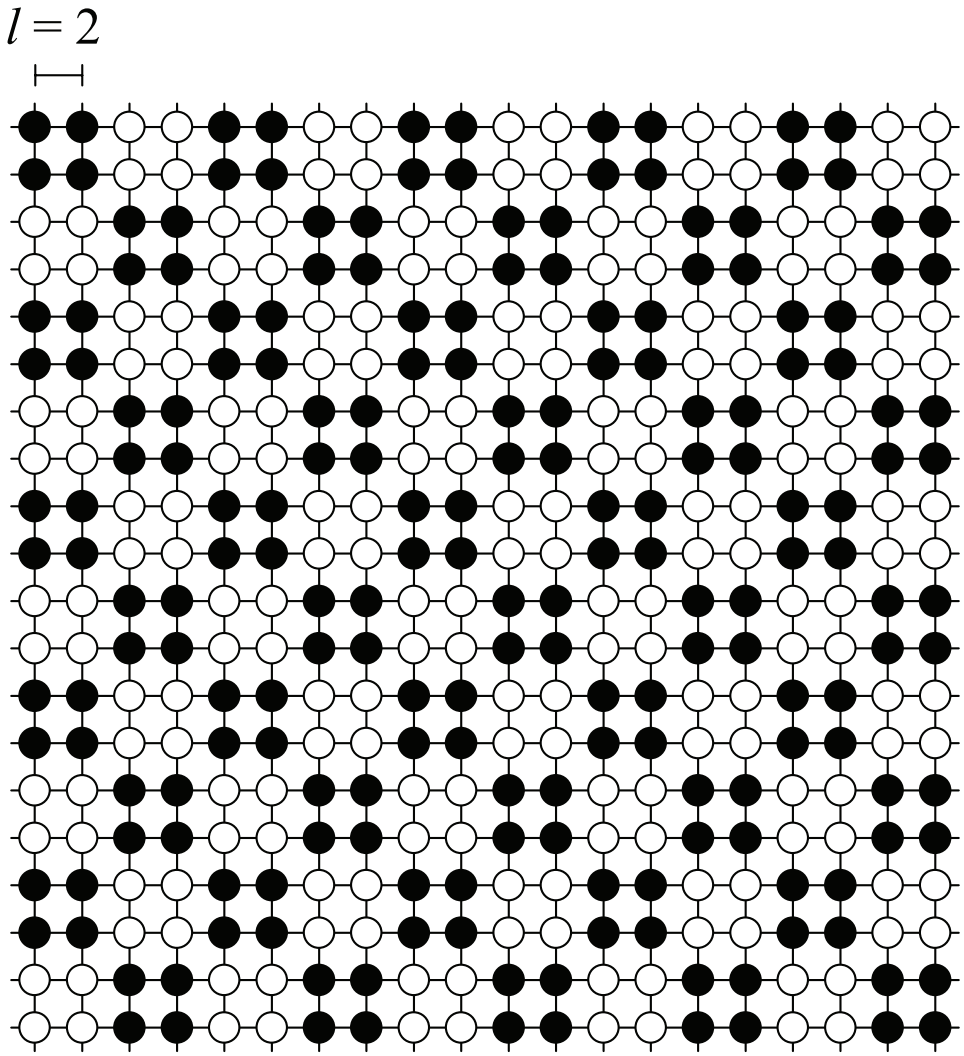

(b)

Fig. 2: Sánchez-Varretti et al.

Figure 3

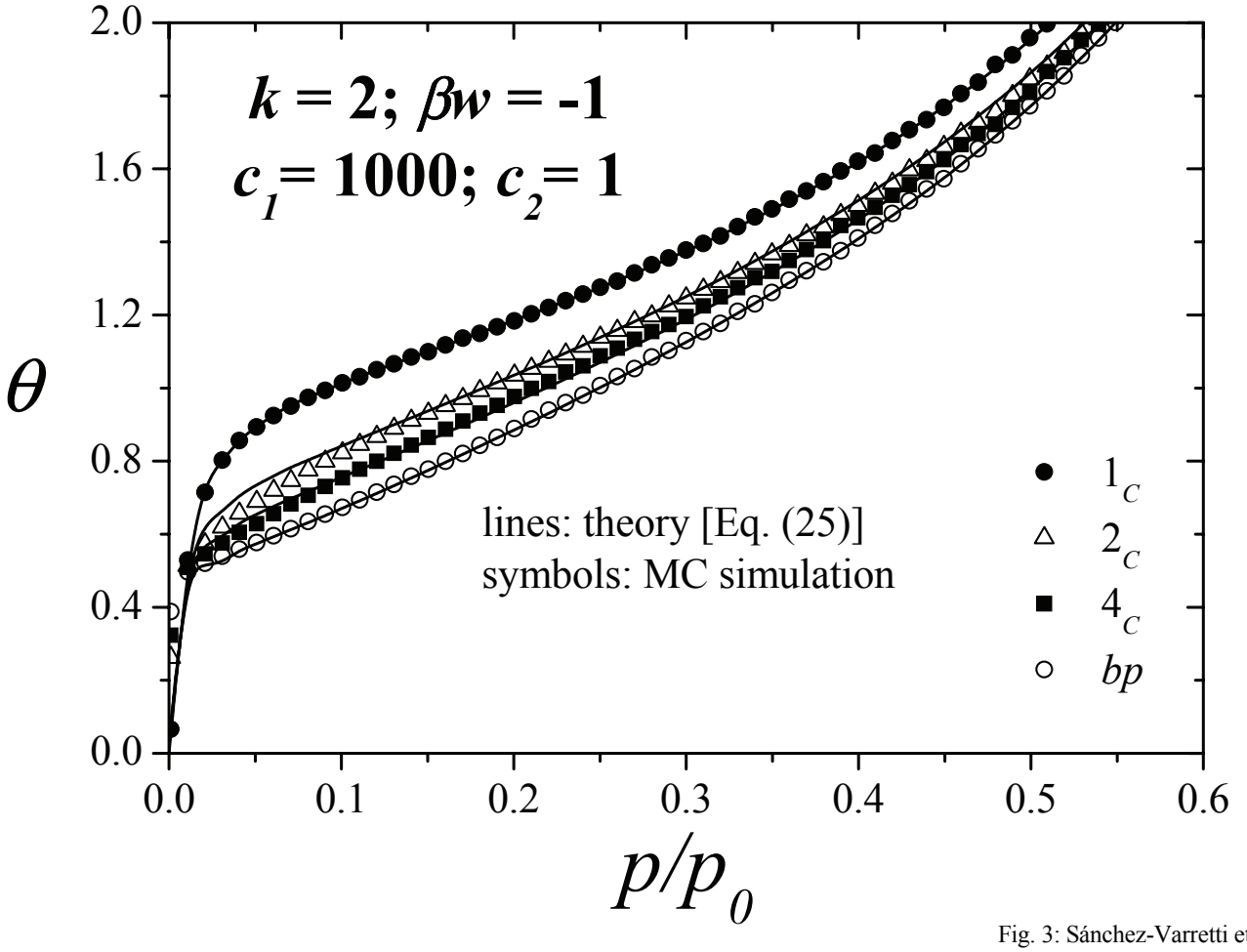

Fig. 3: Sánchez-Varretti et al.

Figure 4

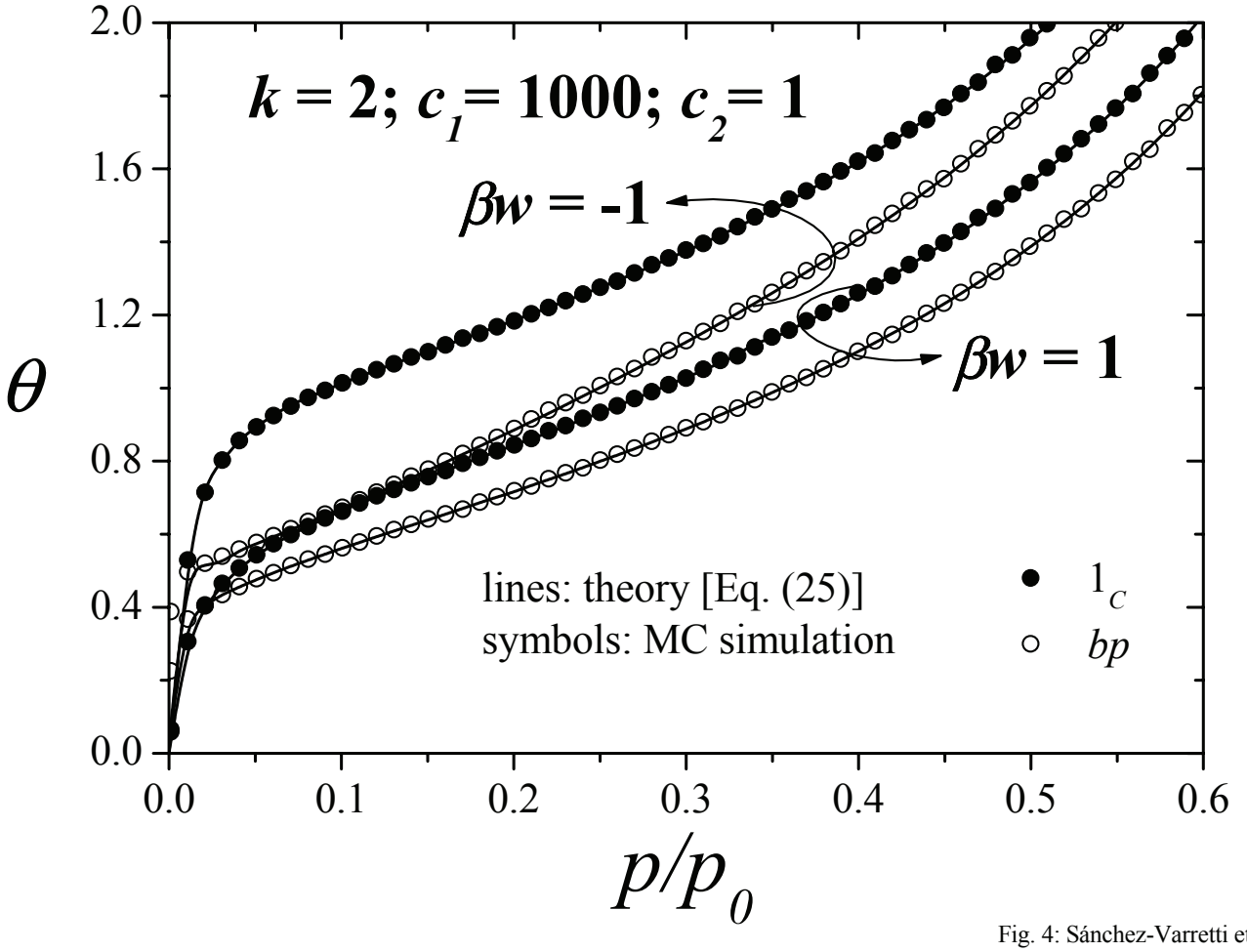

Fig. 4: Sánchez-Varretti et al.

Figure 5

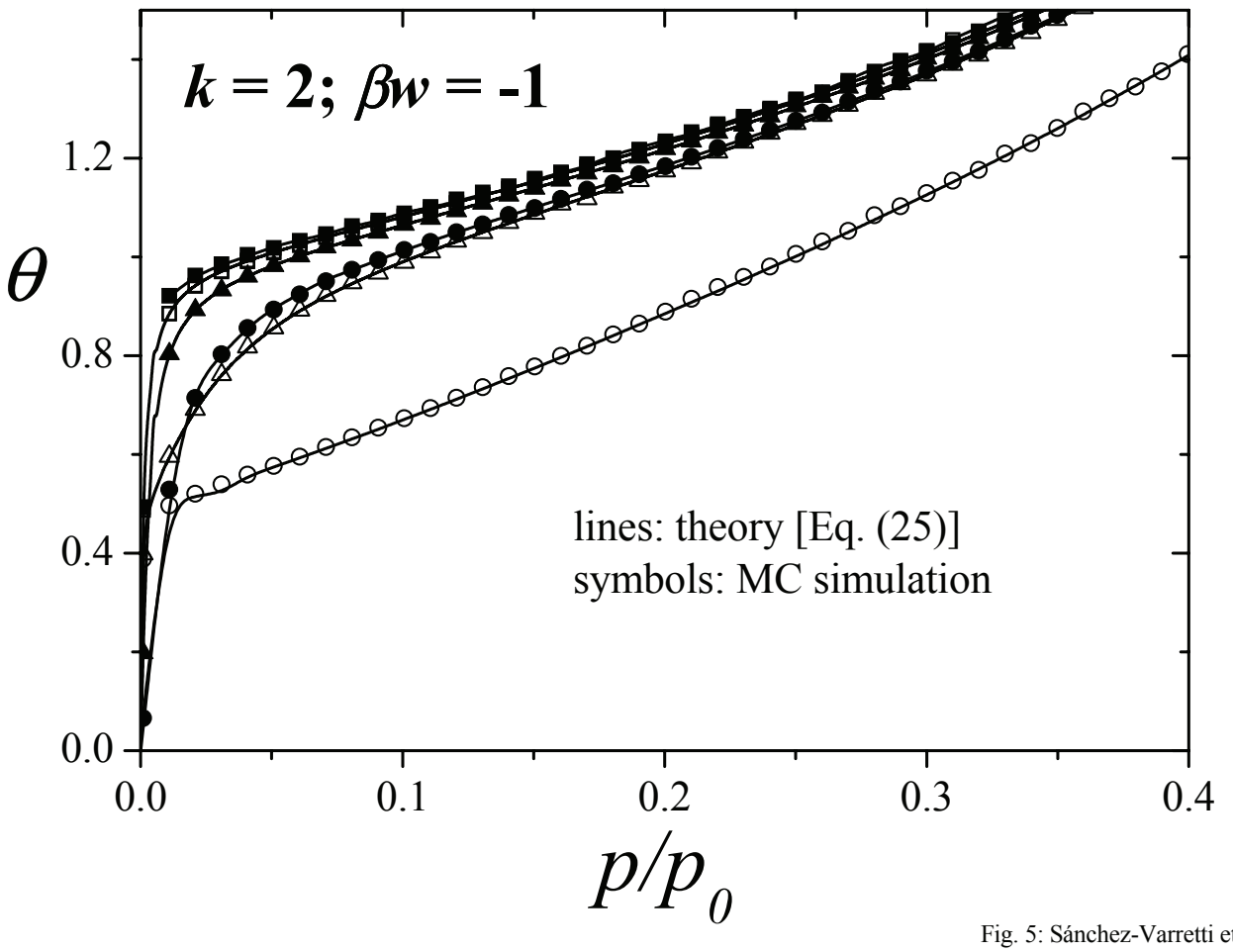

Fig. 5: Sánchez-Varretti et al.

Figure 6

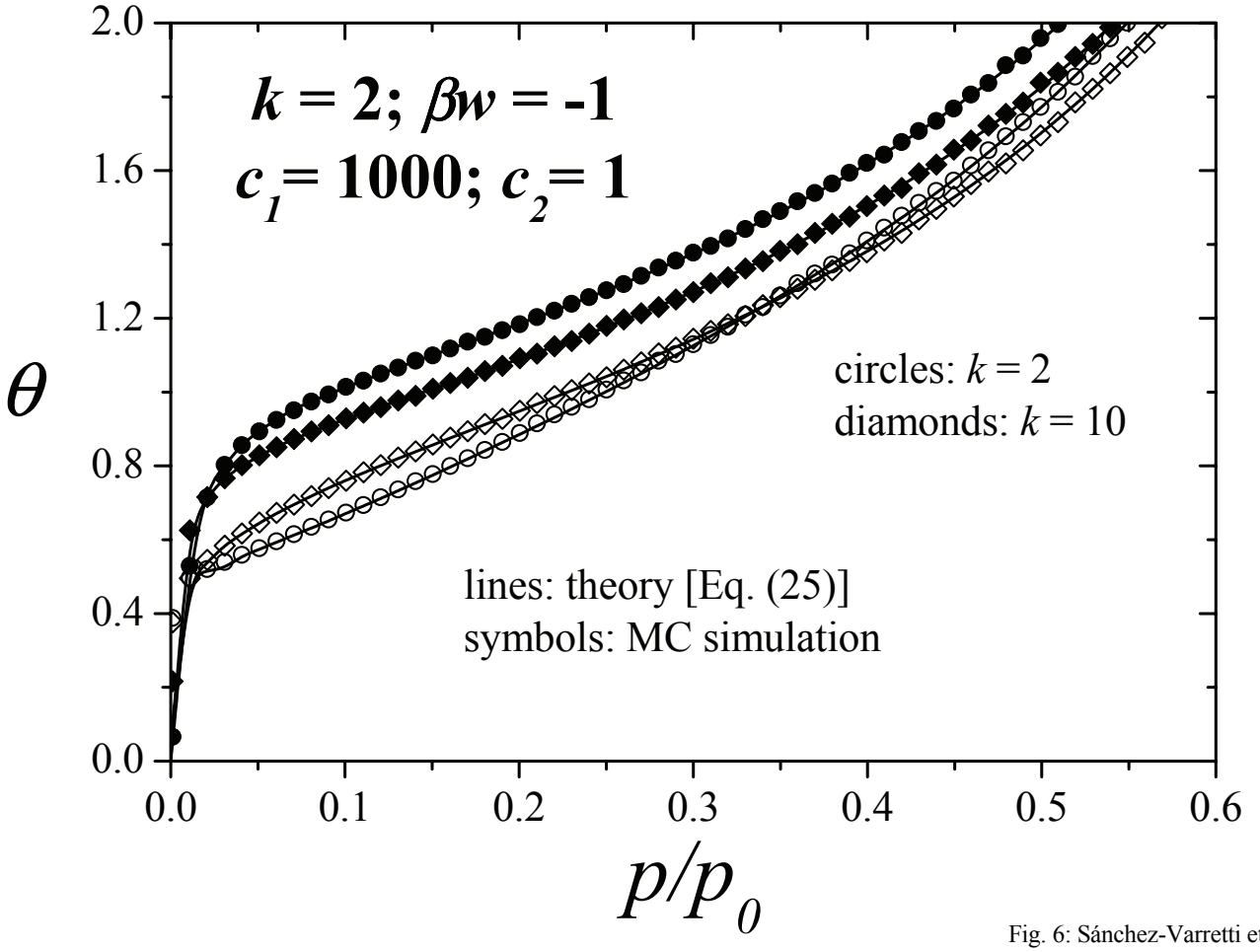

Fig. 6: Sánchez-Varretti et al.

Figure 7

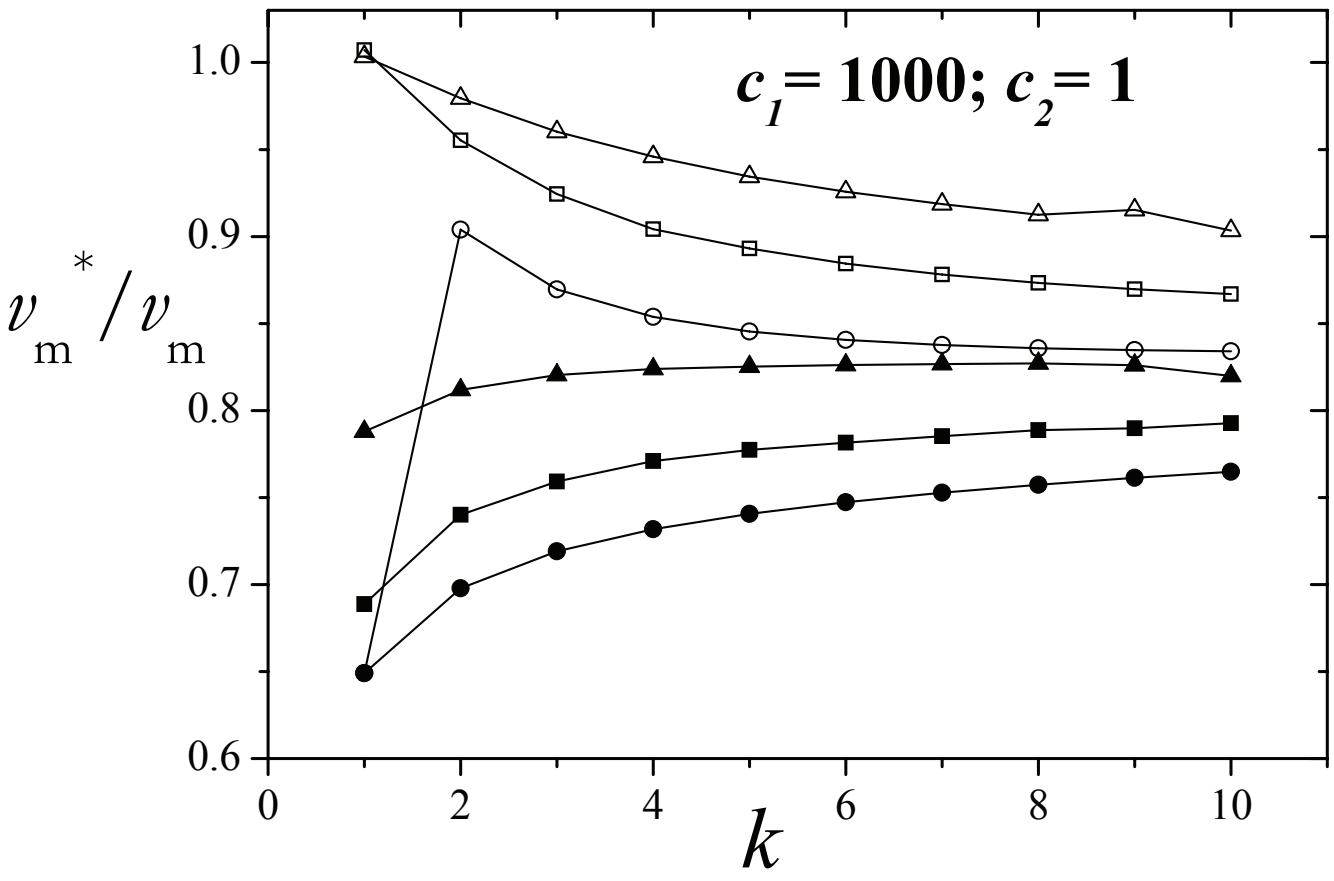

Fig. 7: Sánchez-Varretti et al.

Figure 8

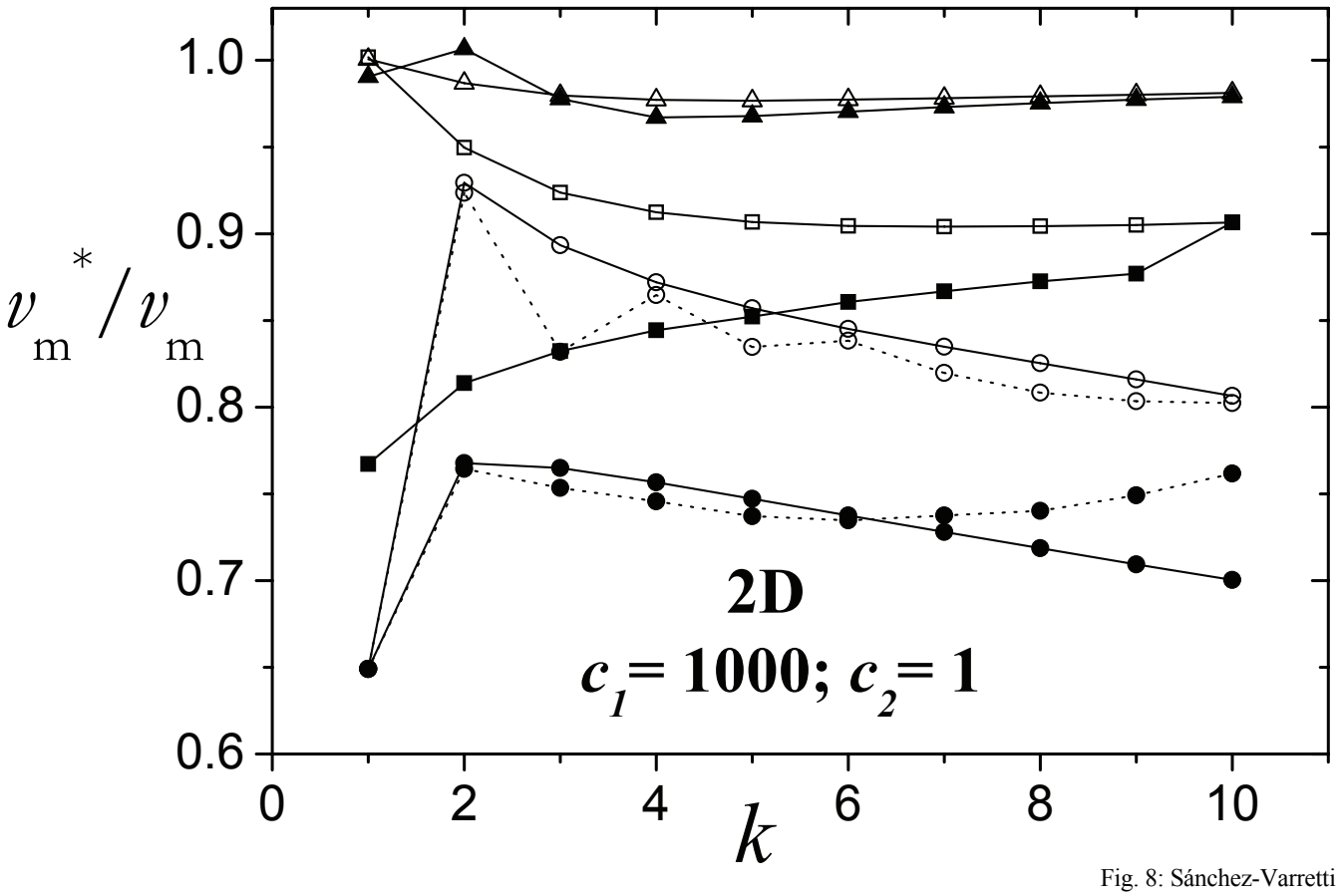

Fig. 8: Sánchez-Varretti et al.